

Single Crystalline Iron Oxide Micrometric Particles with Superparamagnetic Behaviour for MRI Applications

Mihaela Luminita Kiss^{***}, Marius Chirita^{*†}, Corina Ana Beljung^{***}, Robert Polanek^{***}
Cecilia Savij^{****}, Adrian Ieta^{*****}, Alexandru Ionut Mihaila Chirita ^{*****}

*Department of Nanocrystal Synthesis, NIRDECM, Timisoara, Romania;

“Politehnica” University, Timisoara, Romania, *Euromedic Romania Imaging Center, branch
Euromedic Arad, Romania

****Institute of Chemistry Timisoara of Romanian Academy; *****Department of Physics, SUNY
Oswego, NY, USA.

*****University of Vienna, Faculty of Physics, Austria

†corresponding author: Tel/Fax: +40-256-494413, e-mail: chirifiz@gmail.com

ABSTRACT

A major drawback of using metal oxide nanoparticles as contrast agent in MRI is related to their low saturation magnetization, mainly due to their particle size. The current studies seek to solve this problem by increasing the number of nanoparticles in the micrometer sized cluster particles. Studies show that millions of ultrasmall superparamagnetic iron oxide nanoparticles are needed to mark a single cell in order to be effective in improving the MRI signal. However, this approach encounters great challenges. A more suitable solution to this problem could be the use of single micrometer size crystalline particles. Using hydrothermal decomposition of Fe^{3+} - Na_4EDTA complex we synthesized micrometric magnetite single-crystals with average size of $10\mu\text{m}$ (along the $\langle 001 \rangle$ axis) and unusual superparamagnetic behavior at room temperature. Based on our original results on the synthesis of single crystalline micrometric domain (10 - $50\mu\text{m}$) iron oxide (magnetite) with superparamagnetic behaviour **SCMSPIO**, we believe that many interesting applications could follow. Their formulation as T2 contrast agents for MRI may be one of them.

Keywords: MRI, superparamagnetic, magnetite, micrometric, biomedical.

1. INTRODUCTION

Due to the lower rate of diffusion in the tissue as well as due to lower reactivity and weaker interaction with the immune system, microparticles are expected to be safer comparing nanoparticles in the biomedical field. Much effort has been put lately in the synthesis micrometric particles. None of these reports was specifically citing the obtaining of single crystalline microparticles with

superparamagnetic behaviour. Moreover, to our best knowledge, the reported biological research has been performed on magnetite micrometer particles comprising nanoparticle agglomerations.

Several studies have demonstrated that conglomerate superparamagnetic iron oxide-type ultrasmall nanoparticles (USPIO) increased the intensity of the MRI signal [1-5] and improved the monitoring of cellular migration [6-8]. These researches outline the fact that in order to improve the MRI signal several millions of USPIO nanoparticles are necessary to mark a single cell, which is a difficult task [9]. However, Hinds *et al.* [10] have shown that micrometric iron oxide particles (MPIO) can be used as an alternative for the same purpose; such particles may efficiently be endocytosed by various cells. Saphiro *et al.* [9] demonstrated for the first time that a single MPIO particle can be used for cellular marking and then detected by MRI. Therefore, it is estimated that crystalline micrometric particles with superparamagnetic properties could considerably enhance MRI contrast effects. For this reason, findings concerning the design and proceed suitable synthesis methods in order to extend superparamagnetic behaviour from nanometric to micrometric scale constitute a real challenge; they could be extremely useful in environmental and some biomedical applications. Nevertheless, micrometer particle size can be a huge advantage in biomedical applications as they are more secure than the nanoparticles due to the low speed of diffusion in tissue, low reactivity, and low interaction with the immune system. There are only a few reports about synthesis of single crystalline micrometric magnetite in literature but none of them are mentioning superparamagnetic behaviour of the crystals. Soft-magnetic microcrystalline magnetite octahedrons with a size distribution from 4 to $10\mu\text{m}$ have been synthesized by Liu *et al.* [11] through hydrothermal method. The crystals of Liu *et al.* exhibit magnetic properties closely corresponding to

this goal (6.6 emu/g remanence) but the saturation field and the coercivity is 10 kOe and 80 Oe respectively, which is a large value. Moreover, the presented characterization cannot conclude upon synthesized particle monodispersity. Chen *et al.* [12] synthesised octahedral magnetite microcrystals with particle size ranging from 2 to 5 μm with high crystallinity and low coercive field. The magnetic hysteresis loop indicates that the saturation magnetization $M_s = 102.57\text{emu/g}$, remanence magnetization $M_r = 1.44\text{emu/g}$, and coercive field $H_c = 12.55\text{Oe}$, and the reduced magnetization $M_r/M_s = 0.014\text{emu/g}$ which can be qualified as a very good magnetic characteristics. Nevertheless, the saturation field is 10 kOe, which is a large enough value, and the fact there was not about particle monodispersity constitutes a difficulty for use them in medical applications. Jiang *et al.* [13], developed a hydrothermal method to fabricate pseudo-octahedral single crystalline magnetite with size ranging from 5 to 10 μm . The coercivity of the pseudo-octahedral crystals fabricated by Jiang *et al.* is 30 Oe, and its saturation magnetization of 85 emu/g at saturation field of 10 kOe. The authors do not mention anything about the remanence and the particle system morphology characterization. Consequently it was hard to conclude if these particles are monodisperse or not. Deng *et al.* [14] obtained magnetite crystals within micrometer size range, but as in other cases presented, the main disadvantage is that saturation is achieved at a high intensity of field of 9 kOe.

Based on the hydrothermal decomposition of the Fe-EDTA complex in the paper we have reported the successful formation of magnetite monodisperse microcrystals with superparamagnetic behaviour with size of 40-45 μm in specific conditions, mainly based on a relative long treatment duration [15, 16]. We developed also a short time experimental procedure for synthesizing magnetite microoctahedrons in the 10-15 μm range (along the $\langle 001 \rangle$ axis), with superparamagnetic room temperature behavior [17].

In order to contribute to elucidating some issues related to potential applications of these particles in biomedical field, we investigated the possibility of using these particles as MRI contrast agent by running some specific tests.

2. EXPERIMENTAL METHODS

2.1. Synthesis and characterization of the particles

The synthesis and the characterisation of the 10 μm particles was largely presented in the proceeding of Nanotech 2013 [18]. Shortly, an aqueous solution $1.05 \times 10^{-1}\text{M}$ of FAS, $1.05 \times 10^{-1}\text{M}$ Na_4EDTA , $9.71 \cdot 10^{-1}\text{M}$ urea was also prepared. The mixture was transferred into autoclave (teflon-lined stainless-steel) and heated up 2h at 270°C. After cooling, the particles were collected by filtration. The micrometric magnetite was further separated by decantation and magnetic separation. They were washed with bidistilled water and dried at 60°C in air.

The crystal structure of the particles were characterized by

an X'Pert PRO MPD diffractometer (PANalytical) with Cu $K\alpha$ radiation ($\lambda=0.15418\text{nm}$, Ni filter). Using the ICSD (Inorganic Crystal Structure Database) reference code 01-076-1849 we identified the diffraction pattern of magnetite (data not shown). SEM and FEI (Inspect S) were employed for the morphology studies of the particles. The morphology of the magnetite microcrystals representing a combination of octahedral and dodecahedral faces of 10-15 μm in size (along the $\langle 001 \rangle$ axis) is revealed in Figure 1a. Energy-dispersive X-ray spectroscopy (EDAX) analysis was employed for the identification of chemical composition, - Figure 1b. No traces of Na, S, C and N have been observed and only the presence of iron and oxygen is revealed, which confirms the high purity of the magnetite (which although it was confirmed as well by Moessbauer spectroscopy (data not shown). The little bit higher than theoretically predicted O/Fe atomic ratio can be attributed to the hydration and superficial oxidation of magnetite.

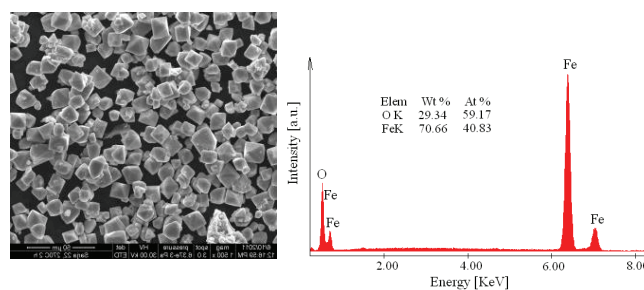


Fig. 1 a) SEM Image, b) Magnetite EDAX spectrum

An AC hysteresigraph [19] was used to test the magnetic properties of the particles. The saturation magnetization (Figure 2) can be estimated to approx. 93 emu/g. The values for coercivity ($H_c=26\text{Oe}$) and magnetic remanence (5emu/g- Fig. 5-inset) are very low, indicating a superparamagnetic-like behavior, which is rather uncommon for the micrometric range of magnetic particles size. The large dispersion in the crystallite axes is consistent with low remanence.

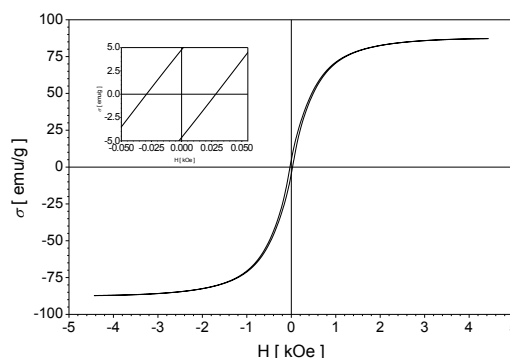


Fig.2. RT magnetic hysteresis loop of the Fe_3O_4 crystals.

Infrared (FTIR) spectrum was recorded in the wave numbers ranging between 4000 and 400 cm^{-1} , with JASCO 4200

Fourier transform infrared (FT-IR) Spectrophotometer using a KBr wafer. The FT-IR spectrum of the particles (figure not presented here) at around 578 cm^{-1} exhibits characteristic bands of substoichiometric magnetite [20, 21]. The FT-IR observed features at 515 cm^{-1} could be considered as characteristic bands of magnetite [22]. A wide and strong band at $3100\text{--}3630\text{ cm}^{-1}$ centred at 3461 cm^{-1} could be assigned to O–H vibrations [23,24] or to adsorbed water molecules [25, 26], which is consistent with EDAX findings. The weak peak situated at approximately 2879 cm^{-1} could be attributed to symmetric C–H vibrations [27]. According Lu the peak at 1632 cm^{-1} may also show the existence of Fe–O (1624 cm^{-1}) [28], or could be a signal of EDTA carboxyl groups when bound to surfaces, [29]. The 1397 cm^{-1} IR feature could be due to vs (COO⁻) as Nowak and co-workers observed [30].

2.3 Preparation of the phantoms

The particles were suspended by ultrasound mixing in a specific gel, a magnetic inert medium which ensure suspension homogeneity and stability. The mixture was loaded in 1,5 ml eppendorf tubes. In order to learn about finding the the correct concentration which gives the optimum MRI signal we prepared three series of samples (phantoms), named GI, GII and GIII, each series containing 10 samples with variable concentrations, decreasing from C1... to Cn.

2.4 MRI apparatus

Images were obtained using MRI device model SIGNA MR / I 1.5 T EXCITE HD, Series no. E4417, manufactured at General Electric Company. All the phantoms were analysed after they were placed in the head antenna.

3. RESULTS AND DISCUSSION

3.1 Obtaining of the Particles

We developed an experimental procedure capable of synthesizing monodisperse magnetite microoctahedrons with $10\mu\text{m}$ in size (along the $\langle 001 \rangle$ axis), by hydrothermal decomposition of the Fe(III)EDTA complex in the presence of urea. The saturation magnetization of the sample estimated at 93 emu/g (at 3.8 kOe), and the low values of both coercivity ($H_c = 26\text{ Oe}$) and magnetic remanence (5 emu/g) suggest a nearly superparamagnetic behaviour, pointing that it was unusual value for magnetic particles of micrometric range sizes. We can conclude that our experimental procedure consists in associating for the first time of superparamagnetic behaviour at ordinary temperature with a micrometric-sized magnetite particle.

3.2 MRI Tests

The main objective for GI series was to determine the concentration that gives a signal close to the undiluted gadolinium reference. These phantoms were placed in the MRN head antenna and were submitted to MRN RF signal. The image in Figure 3 shows three representative phantoms of GI. The results are shown in Fig. 3 a, b, c. Note that the images in Fig. 3a and 3b show artefacts due to high intensity magnetic response of the particles. Best contrast image was in the case presented Figure 3c, where the concentration of microparticles was C1. On a careful examination, the air bubbles can be observed in the gel, which means there is the concrete possibility that in an appropriate environment, and a well-defined concentration, **SCMSPIO** particles can generate a suitable response. For comparison each image presents one eppendorf tube containing pure gel (left) and one eppendorf tube filled with gadolinium contrast agent (right).

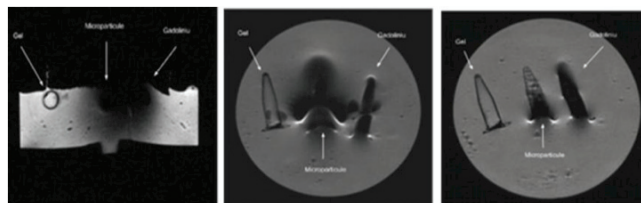


Fig.3 a. b. c.

We chose the C1 concentration as the start point for preparing G II series of 10 phantoms having decreased concentrations. This time, water was chosen as reference. The G II series of phantoms were placed in the MRN head antenna and ware submitted to MRN RF signal.

The main purpose for G II series of experiments was to obtain the images lowest level of distortions. It was observed that the appropriate concentration was C2 (Figure 4a).

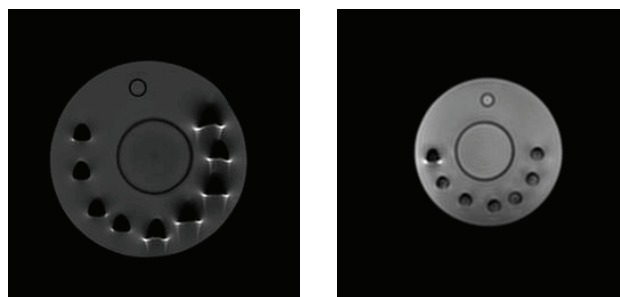


Figure 4. a) b)

Referring to C2 concentration, G III series of phantoms was prepared, having also decreased concentration. At this time we are looking for the darkness of the grey nuances, Figure 4b. Deeper darkness means better contrast appearance.

4. CONCLUSION

Single crystals of Fe₃O₄ with micrometric dimensions of 10µm and superparamagnetic behaviour were synthesized. Our procedure was based by hydrothermal decomposition of the Fe(III)-EDTA complex in the presence of urea and the main precursors are ferric ammonium sulphate and Na₄EDTA.

We tested these particles as contrast agent in MRI experiments and at this stage of experiments the nuances of grey which we obtained show promising effects and they correspond to our expectations. The results indicate that the choice of appropriate concentration might give a good contrast in MRI applications. Further *in vivo* experiments on animals are in progress.

Taking into account the dimensions of the cells (10µm - 100µm), these particles could be appropriate for the use in other medical applications such as intracellular hyperthermia, controlled drug delivery system (site specific drug delivery), cellular Magnetic Resonance Imaging (MRI), monitoring cell migration for cell therapy, multimodal cancer therapy, immune-magnetic separation of cells, detection, immobilization and modification of biologically active compounds, cell labelling; magnetic separation of cells, magnetic resonance contrast agents, gene delivery, multi-modal cancer therapy.

ACKNOWLEDGEMENTS

This work was supported by program PN 09 34 01 01 of the Ministry of Research and Education in Romania. We address many thanks to Euromedic Romania Imaging Center, branch Euromedic Arad, Romania, for technical supporting.

REFERENCES

- [1] G.M. Lanza, D.R. Abendschein, X. Yu, P.M. Winter, K.K. Karukstis, M.J. Scott, R. W. Fuhrhop, D.E. Scherrer, S. A. Wickline, *Academic Radiology*, 9 Suppl. 2:S330–S331, 2002.
- [2] P. F. Renshaw, C. S. Owen, A. E. Evans, J. S. Leigh Jr., *Magnetic Resonance Imaging*, 4, 4, 351–357, 1986.
- [3] S.A. Anderson, R.K. Rader, W.F. Westlin, C. Null, D. Jackson, G.M. Lanza, S.A. Wickline, J. J. Kotyk, *Magnetic Resonance in Medicine*, 44, 3, 433–439, 2000.
- [4] H. Gupta, R. Weissleder, *Magnetic Resonance Imaging Clinics of North America*, 4, 1, 171–84, 1996.
- [5] C.P. King, M.D. Li, M.D. Bednarski, *Journal of Magnetic Resonance Imaging*, 16, 4, 388–393, 2002.
- [6] J.W.M. Bulte, S.C. Zhang, P. Gelderen, V. Herynek, E. K. Jordan, I. D. Duncan, J.A. Frank, *Proceedings of the National. Academy of Sciences*, 96, 15256–15261, 1999.
- [7] M. Modo, D. Cash, K. Mellodew, S.C.R. Williams, S.E. Fraser, T.J. Meade, J. Price, H. Hodgesn, *NeuroImage*, 17, 2, 803–811, 2002.
- [8] M. Hoehn, E. Küstermann, J. Blunk, D. Wiedermann, T. Thorsten, S. Wecker, M. Föcking, H. Arnold, J. Hescheler, B.K. Fleischmann, W. Schwindt, C. Bührle, 99, 16267–16272, 2002.
- [9] E. M. Shapiro, S. Skrtic, K. Sharer, J. M. Hill, C.E. Dunbar, A. P. Koretsky, 101, 30, 10901–10906, 2004.
- [10] K.A. Hinds, J.M. Hill, E.M. Shapiro., et al. *Blood*. 102 867–872, 2003.
- [11] Liu X.M., Fu S.Y., Xiao H.M., *Mater. Lett.* 60, 2979–2983, (2006).
- [12] Haiping Qi, JingYe, NanTao, MinghuaWen, Qianwang Chen, *Journal of Crystal Growth* 311 (2009) 394 – 398.
- [13] Ming Hu, Rui-Ping Ji, Ji-Sen Jiang, *Materials Research Bulletin* 45 (2010) 1811–1815
- [14] H. Deng, X. Li, Q. Peng, X. Wang, Chen, Li Y., *Angew. Chem.*, 44, 2782, 2005.
- [15] M. Chirita, A. Ieta, *Cryst. Growth Des.* 12.2:883–886, 2012.
- [16] M. Chirita, R. Banica, A Ieta, I. Grozescu, *Particul Sci Technol.* 30 354–363, 2012.
- [17] M. Chirita, R. Banica, P. Sfarloaga, A. Ieta, and I. Grozescu. *IEEE Conference Proceedings* October 11–13, Sinaia, Romania, vol. 2, pp. 391–394, 2010.
- [18] M. Chirita, M. L. Kiss, A. Ieta, A. Ercuta, I. Grozescu *NTSI-Nanotech 2013*, ISBN 978-1-4822-0581-7 Vol 1, 2013.
- [19] I. Mihalca, A. Ercuta, “*Journal of Optoelectronics and Advanced Materials* 5.1, pp. 245 – 250, 2003.
- [20] U. Schwertmann and R. M. Cornell, NY: Wiley, 2000.
- [21] M. Gotic and S. Music, *Journal of Molecular Structure* 834–836 p. 445–453, 2007.
- [22] D. Zhao, X. Wu, and H. G. E. Han, *J. Supercrit. Fluids* 42 p 226–233, 2007.
- [23] C. Claudia Wagner and J. Enrique Baran, *Spectrochimica Acta Part A* 75 p. 807–810, 2010.
- [24] M. Tsai Liang, S. Han Wang, Y. Lun Chang, H. I. Hsiang, H. Jhe Huang, M. Huan Tsai, W. Cheng Juan, and S. Fu Lu, *Ceramics International* 36 p. 1131–1135, 2010.
- [25] A. Bocanegra Diaz, N. D. S. Mohallem, and R. D. Sinisterra. *J. Braz. Chem. Soc.* 14, 936–941, 2003.,
- [26] Z. L. Liu, X. Wang, K. L. Yao, G. H. Du, Q. H. Lu, Z. H. Ding, J. Tao, Q. Ning, X. P. Luo, D. Y. Tian, and D. Xi, *J. Mater. Sci.* 39 p. 2633–2636, 2004.
- [27] C. Yu Wang, J. Ming Hong, G. Chen, Y. Zhang, and N. Gu, *Chinese Chemical Letters* 21 p. 179–182, 2010.
- [28] W. Lu, Y. Shen, A. Xie, and W. Zhang, *J. Magnetism and Magnetic Materials* 32 p. 1828–1833, 2010.
- [29] Z. Li, H. Chen, and M. Gao, *Chem. Mater.* 16 p. 1391–1393, 2004.
- [30] B. Nowack, J. Lutzenkirchen, P. Behra, and L. Sigg, *Environ. Sci. Technol.* 30 p. 2397–2405, 1996.